



OPEN Bose glass and Fermi glass

Korekiyo Takahashi^{1,2,6}✉, Keiji Nakatsugawa^{2,5,7}, Masahito Sakoda^{1,2}, Yoshiko Nanao³, Hiroyoshi Nobukane^{2,4}, Hideaki Obuse^{1,2,7} & Satoshi Tanda^{1,2,7}

It is known that two-dimensional superconducting materials undergo a quantum phase transition from a localized state to superconductivity. When the disordered samples are cooled, bosons (Cooper pairs) are generated from Fermi glass and reach superconductivity through Bose glass. However, there has been no *universal* expression representing the transition from Fermi glass to Bose glass. Here, we discovered an experimental renormalization group flow from Fermi glass to Bose glass in terms of simple β -function analysis. To discuss the universality of this flow, we analyzed manifestly different systems, namely a Nd-based two-dimensional layered perovskite and an ultrathin Pb film. We find that all our experimental data for Fermi glass fall beautifully into the conventional self-consistent β -function. Surprisingly, however, flows perpendicular to the conventional β -function are observed in the weakly localized regime of both systems, where localization becomes even weaker. Consequently, we propose a universal transition from Bose glass to Fermi glass with the new two-dimensional critical sheet resistance close to $R_{\square} = h/e^2$.

The electric conductance in the quantum localized regime (a regime where the electrical resistance increases as the temperature decreases) of two-dimensional (2D) disordered systems has been discussed in terms of Fermi glass^{1–7}, i.e., Mott localization^{8,9} for strongly correlated systems and Anderson localization^{10–15} for non-interacting systems¹⁶, and Bose glass^{17,18}. The Bose glass phase is an insulator phase with properties similar to those of Fermi glass, and can be described as the phase where the 2D bosons are localized as a result of the quenched 2D disorder. Anderson localization has been studied using β -function analysis^{10,19}. Mott localization has been studied via Mott variable range hopping conduction (VRH)²⁰ and via Fisher scaling for the boson Hubbard model^{8,21,22}. Recently, Kapitulnik *et al.*²³ have shown that there is an anomalous metal state that overturns the conventional wisdom in the regime below the superconducting critical sheet resistance^{8,24} $h/4e^2$ and is different from the quantum localized regime. However, a boson-fermion mixture or a transition from Fermi glass to Bose glass has not been considered in the quantum localized regime.

In this Article, we discovered an experimental renormalization group flow from Fermi glass to Bose glass in terms of β -function analysis. The critical sheet resistance, which is the boundary between Bose glass and Fermi glass, is indicated to be around h/e^2 as shown in Fig. 1.

To discuss the universality of this flow, we analyzed manifestly different systems, namely a Nd-based two-dimensional layered perovskite and an ultrathin Pb film. The layered perovskite structure of Nd₂CuO₄ and Nd₂PdO₄ is called a T' -structure²⁵, and it has an ideal 2D electron conductance because the conducting layer is composed of square planar units. FIG. 2 shows the temperature dependence of the electric resistance for Nd₂CuO_{4–x}F_x single crystals²⁶, Nd_{2–x}Ce_xCuO₄ thin films²⁷, and Nd_{2–x}Ce_xPdO₄ thin films²⁸. Doping causes a Nd₂CuO₄ system to undergo a quantum phase transition from the localized state to the superconducting state, i.e., superconductivity–insulating (S–I) transition. Superconductivity is not observed in a Nd₂PdO₄ system regardless of the doping amount²⁸. On the other hand, the ultrathin Pb film²⁹ is grown sequentially in situ by the evaporation of Pb. The film changes to a superconductor from an insulator as the film thickness increases (Fig. 2).

We find that all experimental data in Fermi glass fall beautifully into the conventional self-consistent β -function. Surprisingly, however, flows perpendicular to the conventional β -function were observed in the weakly localized regimes of both systems, where localization becomes even weaker. We show that the perpendicular flow implies the existence of Bose glass by using an experimental β -function and the temperature-derivative equation of the β -function (β' -function). Consequently, we can propose that there is a universal transition from Bose glass to Fermi glass with the new two-dimensional critical sheet resistance close to $R_{\square} = h/e^2$. Since the Bose glass phase in two types of Nd-based two-dimensional layered perovskites and Pb ultrathin films both exhibit

¹Department of Applied Physics, Hokkaido University, Sapporo 060-8628, Japan. ²Center of Education and Research for Topological Science and Technology, Hokkaido University, Sapporo 060-8628, Japan. ³School of Physics and Astronomy, University of St Andrews, Fife KY16 9SS, Scotland. ⁴Department of Physics, Hokkaido University, Sapporo 060-0810, Japan. ⁵Research Center for Materials Nanoarchitectonics, National Institute for Material Science, Tsukuba 305-0044, Japan. ⁶Nomura Research Institute, Ltd., Tokyo 100-0004, Japan. ⁷These authors contributed equally: Keiji Nakatsugawa, Hideaki Obuse and Satoshi Tanda. ✉email: korere@gmail.com

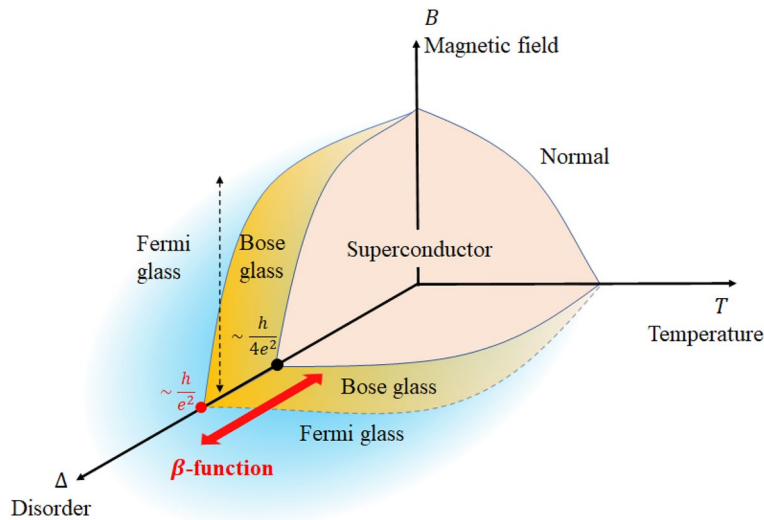


Figure 1. Schematic phase diagram for 2D disordered superconducting materials. The analysis in this article used the β -function to show the behavior of the change from Bose glass to Fermi glass before reaching superconductivity (bi-directional red arrow). The critical sheet resistance, which is the boundary between Bose glass and Fermi glass, is indicated to be around h/e^2 (red dot). The bi-directional black dotted arrow represents Paalanen et al.'s experiments¹⁸.

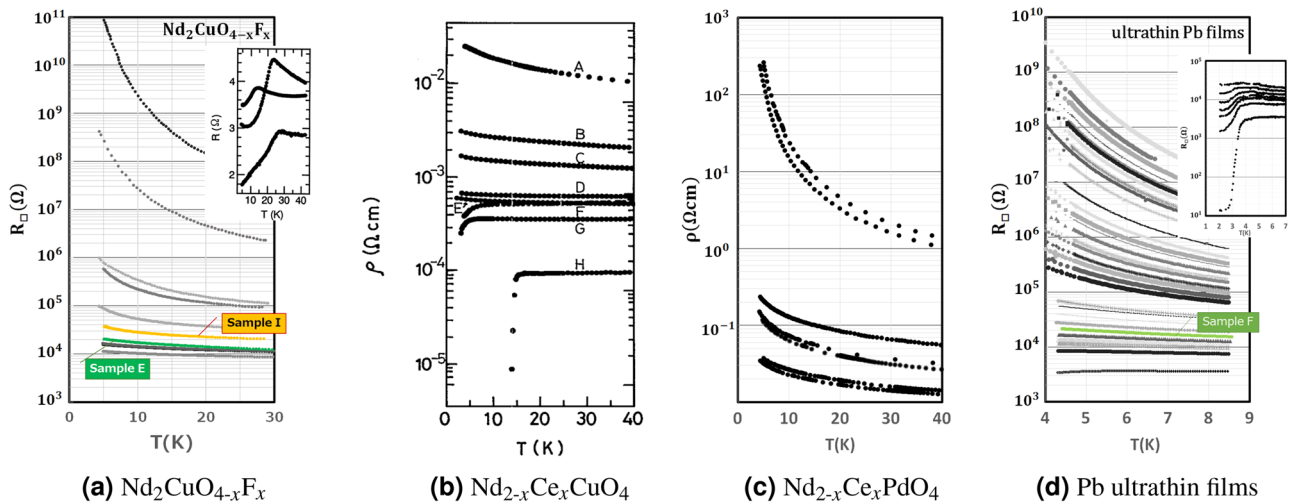


Figure 2. The temperature dependence of the electric resistivity (a) $\text{Nd}_2\text{CuO}_{4-x}\text{F}_x$ ²⁶, (b) $\text{Nd}_{2-x}\text{Ce}_x\text{CuO}_4$ ²⁷, (c) $\text{Nd}_{2-x}\text{Ce}_x\text{PdO}_4$ ²⁸ and (d) ultrathin Pb films²⁹ (thickness changed from 13.8 Å to 42.8 Å). Superconductivity–insulator transition is observed in (a) $\text{Nd}_2\text{CuO}_{4-x}\text{F}_x$ (the inset shows the superconducting state), $\text{Nd}_{2-x}\text{Ce}_x\text{CuO}_4$ and (d) ultrathin Pb films (the inset shows the superconducting state), while in (c) $\text{Nd}_{2-x}\text{Ce}_x\text{PdO}_4$ only the insulating state appears. Sample E of $\text{Nd}_2\text{CuO}_{4-x}\text{F}_x$, Sample I of $\text{Nd}_2\text{CuO}_{4-x}\text{F}_x$ and Sample F of ultrathin Pb films will be discussed in detail later. Sample E of $\text{Nd}_2\text{CuO}_{4-x}\text{F}_x$ is shown to be Bose glass and Sample I of $\text{Nd}_2\text{CuO}_{4-x}\text{F}_x$ is shown to be Fermi glass. Sample F of ultrathin Pb films shows a change from Fermi glass to Bose glass as the temperature becomes lower.

a β' -function different from that of the Fermi glass phase, with R_{\square} between h/e^2 and $h/4e^2$, this phenomenon is considered universal.

Vertical flows in β -function analysis

We investigate our experimental results with β -function analysis^{10,13}, which is applicable from weak to strong localization regimes. The β -function is defined as $\beta(g) \equiv d \ln g / d \ln L$, where L is the sample size, and g is the dimensionless conductance [$g = (\hbar/e^2)\sigma$ in 2D]. The β -function shows the flow of electronic states as a function of size L and can be used to determine whether it is delocalized or localized, and even weakly or strongly

localized. In other words, if we view the form of the β -function as a renormalization group flow, we can understand the universality of the electronic state with the scale transformation.

Experimentally, L is taken to be the cutoff length due to inelastic scattering: $L^2 = DT^{-p}$. D is the diffusion constant, and T is the temperature. The value of exponent p depends on the inelastic scattering mechanism. For Nd-based 2D layered perovskite systems, $p = 1.0^{26}$. For ultrathin Pb films, $p = 2.1^{29}$. So, the β -function is derived from the experimental data of the temperature dependence of the conductance as follows:

$$\beta_{\text{EXP.}}(g) = -\frac{2}{p} \frac{d \ln g}{d \ln T}. \quad (1)$$

This equation is predicted to behave as follows from weak to strong localized regimes;

In a weakly localized regime, the celebrated weak localization theory in 2D¹³ predicts the logarithmic system size dependence of the dimensionless conductance as

$$g = g_0 - g_1 \ln \left[\frac{L}{l} \right], \quad (2)$$

with a non-universal constant $g_0 = 1/(k_F l)$, where k_F and l are the Fermi wave number and the mean free path, and a universal coefficient $g_1 = 1/\pi^2$. Substituting Eq. (2) into Eq. (1) with the fact that $\ln L = -\frac{p}{2} \ln T$, we obtain the universal scaling relation as follows:

$$\beta_{\text{EXP.}}(g) = -\frac{2}{p} \frac{d \ln(g_0 + g_1 \frac{p}{2} \ln T)}{d \ln T} = -\frac{g_1}{g} = -\frac{1}{\pi^2 g}. \quad (3)$$

Since p is canceled out in the above calculation, $\beta_{\text{EXP.}}(g)$ is related only to g . With a strong localized regime, namely the VRH theory in Mott 2D, $g \propto \exp(-\varepsilon_{\text{VRH}}/T^{1/3})$, so that $\beta_{\text{EXP.}}(g) \sim \ln g$. This ε_{VRH} is equal to the generalized activation energy³⁰.

On the other hand, in the self-consistent theory of the β -function, Vollhardt and Wölfle gave a single 2D system conductivity formula for orthogonal classes from weakly to strongly localized regimes^{31,32}.

$$g_{\text{VW}}(x) = \frac{1}{2\pi^2} (x+1) \ln \left(\frac{1}{x^2} + 1 \right) \exp(-x), \quad (4)$$

Here, $x = L/\xi \propto T^{-p/2}/\xi$, where ξ is the localization length. Furthermore, the β -function from Eq. (4) can be calculated as follows:

$$\beta_{\text{VW}}(g) = \frac{d \ln g_{\text{VW}}(x)}{d \ln x} = - \left(\frac{x^2}{x+1} + \frac{2}{(x^2+1) \ln \left(\frac{1}{x^2} + 1 \right)} \right). \quad (5)$$

We analyzed our experimental data by using the above equations: first, we estimated ξ from Eq. (4). Next we described the β -function obtained from Eq. (5). Finally we overlaid the $\beta_{\text{EXP.}}(g)$ data of Eq. (1) and the $\beta_{\text{VW}}(g)$ data of Eq. (5), to verify whether or not they matched. We see that all the data from weakly to strongly localized regimes fall into $\beta_{\text{VW}}(g)$ (inset of Fig. 3). However, if we take a closer look at the weakly localized regime, as shown in Fig. 3, we discover that the data exhibit different *perpendicular flows* (indicated by the red arrows) against the usual Anderson localization β -function curve (indicated by the blue arrows). In the weakly localized regime, these perpendicular flows are present in both Nd-based 2D layered perovskite and ultrathin Pb films. In some ultrathin Pb film samples, it is clear that the flow changes from the usual Anderson localization flow to the perpendicular flow at a certain temperature (e.g., Pb-sample-F surrounded by a dotted circle). Nd₂CuO_{4-x}F_x single crystals and Nd_{2-x}Ce_xCuO₄ thin films have different perpendicular flows, but Nd_{2-x}Ce_xPdO₄ does not have them. It is considered to be a phenomenon that is a precursor to the transition from weak localization to superconductivity. The discovery of the upturn from the $\beta_{\text{VW}}(g)$ to the perpendicular flow suggests that the single parameter hypothesis is not sufficient³³⁻³⁶. However, this β -function analysis method will suggest us to understand the causes and the conditions of these perpendicular flows.

To understand the mechanism of perpendicular flows, we again analyze the temperature dependence of resistivity in more significant detail. The functional forms of these perpendicular flows appear in the weakly localized regime but are not adapted to $-1/g$. Therefore, we analyzed two samples before and after the perpendicular flow occurred; namely (a) Nd₂CuO_{4-x}F_x (NCOF) sample E in which this perpendicular flow appears and (b) NCOF sample I in which the perpendicular flow does not appear. As a result, we find a difference in the temperature dependence of conductivity σ and resistivity $\rho (= 1/\sigma)$. As shown in Fig. 4, the $\ln T$ dependence of the NCOF-sample-E resistivity is more suitable than that of the conductivity. In contrast, according to the Anderson localization theory, the NCOF-sample-I conductivity has $\ln T$ dependence. Although these are in the same weakly localized regime, the perpendicular flow is clearly characterized by $\rho \sim \ln(1/T)$ rather than by $\sigma \sim \ln T$.

Das et al.³⁷ pointed out that the weak localization of bosons occurring on the insulator side of the S-I transition in 2D is characterized by $\rho \sim \ln(1/T)$. Therefore, the state of the sample with the perpendicular flow can be regarded as boson localization or the Bose glass phase. These experimental results indicate that the Bose glass regime has been found.

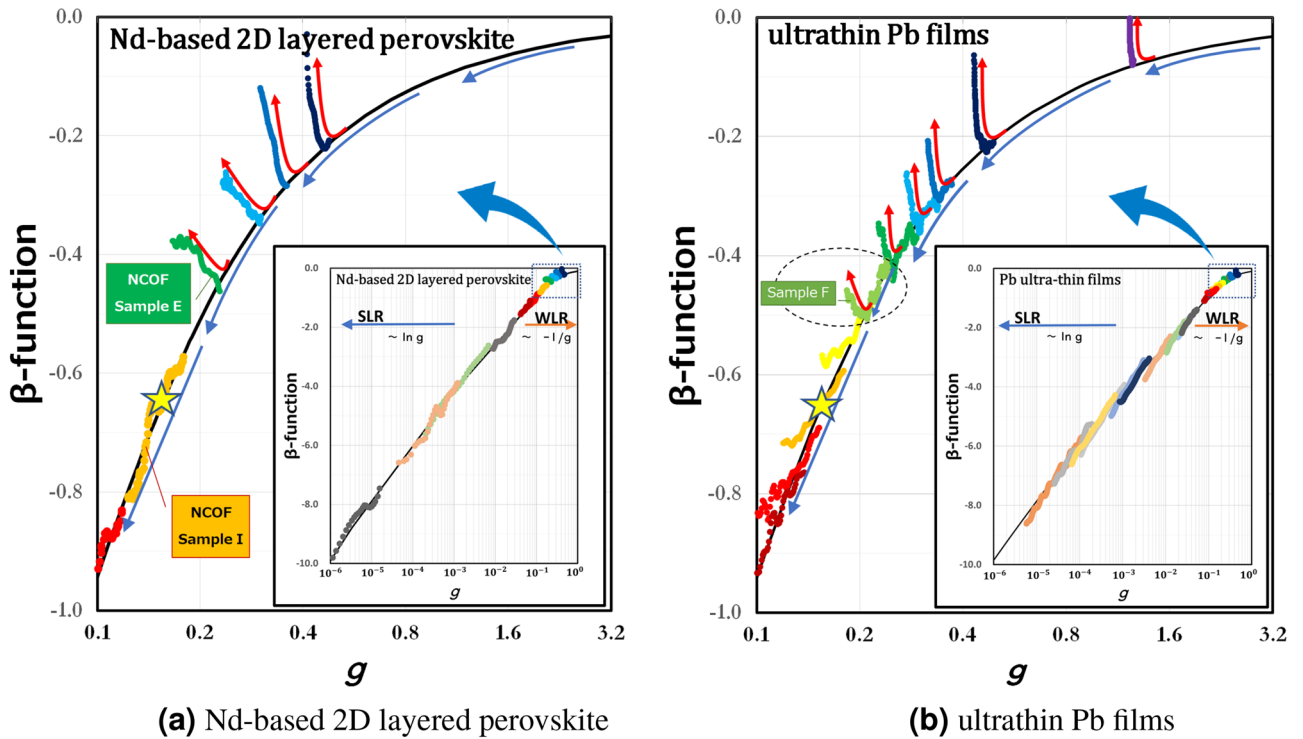


Figure 3. Enlarged view of $\beta_{\text{EXP}}(g)$ - the experimental β -function in a weakly localized regime. The inset shows $\beta_{\text{EXP}}(g)$ from a weak to a strong localized regime. The solid black line shows $\beta_{\text{VW}}(g)$ — Vollandt and Wölfle β -function [(eq. (5))]. The data for Nd-based 2D layered perovskite were plotted using resistance values from 5 to 25 K. The data for ultrathin Pb films were plotted using resistance values from 4 to 10 K. The color depends on the sample. If we view the β -function as a renormalization group flow, the Anderson localization β -function flow should behave like $\beta_{\text{VW}}(g)$, as indicated with the blue arrows. However, as shown by the red arrows, we discover a different flow which is perpendicular to $\beta_{\text{VW}}(g)$. In the weakly localized regime, these flows are present in both systems. In some ultrathin Pb film samples (e.g., Pb-sample-F surrounded by a dotted circle), it is clear that the flow changed from the usual Anderson localization flow to a perpendicular flow at a certain temperature. The yellow star in each graph indicates $g = 1/2\pi$ and $\beta = -2/\pi$, which is the dimensionless version of the critical sheet fermion resistance $R_{\square} = h/e^2$. This star is the boundary value at which the perpendicular flow occurs, as determined from Fig. 5 and Appendix B. Therefore, it proves that the phenomenon of these perpendicular flows is at its least apparent when R_{\square} is smaller than h/e^2 .

The transition from Fermi glass to Bose glass

Next, to investigate the change condition from Bose glass to Fermi glass, we plotted the temperature dependence of $\beta_{\text{EXP}}(g)$ instead of the resistance, as shown in Fig. 5 with a series of experimental data. Interestingly, the temperature dependence of $\beta_{\text{EXP}}(g)$ in the weakly localized regime is very similar to the S–I transition graph. As the localization of each sample weakens (from the bottom to the top of Fig. 5), the slope of each set of data changes continuously from positive to negative in both Nd-based 2D layered perovskite and ultrathin Pb films.

To understand the change in the slope of $\beta_{\text{EXP}}(g)$ flows in Fig. 5, we use the temperature-derivative equation of the β -function shown below,

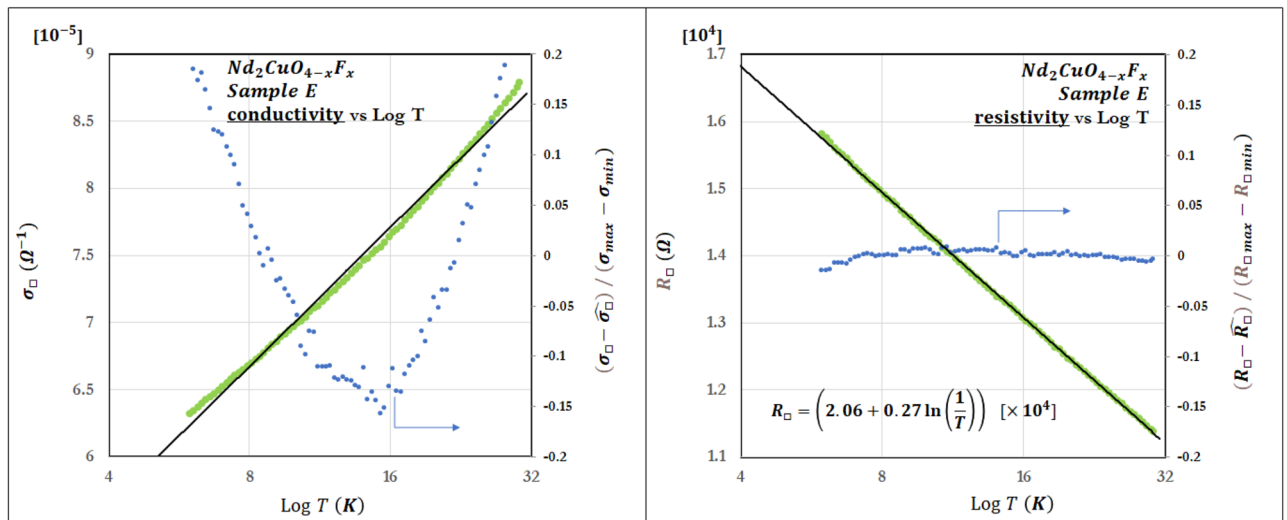
$$\beta'_{\text{EXP}}(g) = -\frac{d \ln |\beta_{\text{EXP}}(g)|}{d \ln T}. \tag{6}$$

The change in the β -function flow should appear in the positive or negative sign of $\beta'_{\text{EXP}}(g)$. Substituting the two equations $\sigma = \sigma_0 + \sigma_1 \ln T$ and $\sigma = 1/\rho = 1/(\rho_0 + \rho_1 \ln(1/T))$ ($\sigma, \sigma_0, \sigma_1, \rho_0, \rho_1 > 0$) we see that the signs are different as follows.

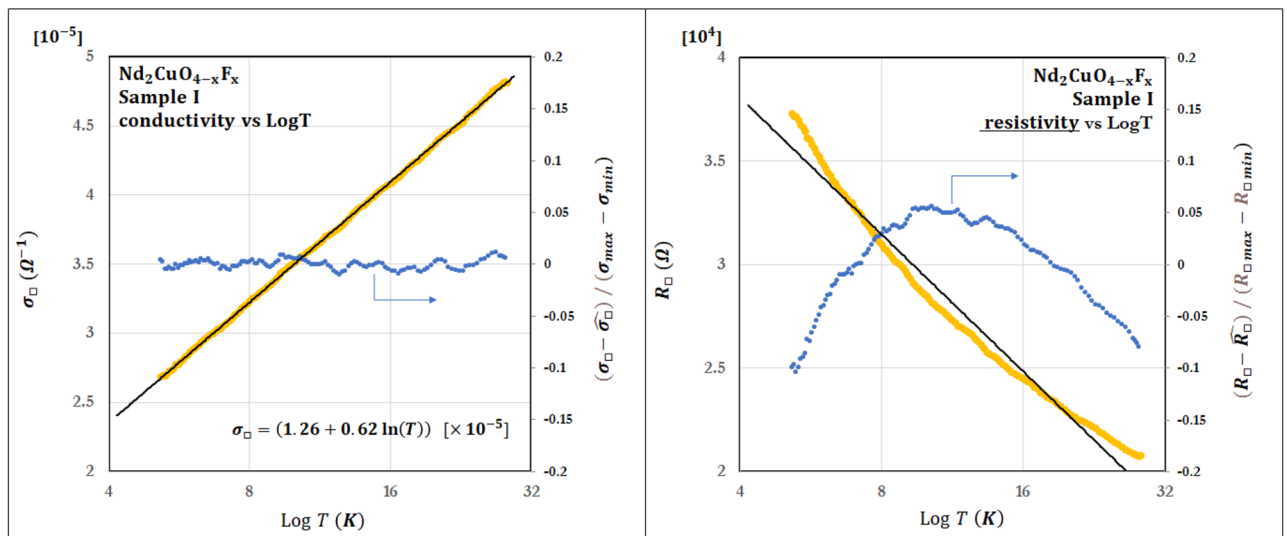
$$\beta'_{\text{EXP}}(g) = \frac{\sigma_1}{\sigma_0 + \sigma_1 \ln T} > 0, \quad (\sigma = \sigma_0 + \sigma_1 \ln T) \tag{7}$$

$$\beta'_{\text{EXP}}(g) = -\frac{\rho_1}{\rho_0 + \rho_1 \ln(1/T)} < 0, \quad (\sigma = \frac{1}{\rho} = \frac{1}{\rho_0 + \rho_1 \ln(1/T)}). \tag{8}$$

In the above calculations, we treat σ as g . While the σ has a dimensionality, this does not change the sign of $\beta'_{\text{EXP}}(g)$. These calculation results confirm that the slope of $\beta_{\text{EXP}}(g)$ reflects the temperature-dependent functional form of the conductivity and resistivity. To check this, we analyzed all the data for $\beta'_{\text{EXP}}(g) < 0$ and found



(a) $\text{Nd}_2\text{CuO}_{4-x}\text{F}_x$ Sample E in the Bose glass regime



(b) $\text{Nd}_2\text{CuO}_{4-x}\text{F}_x$ Sample I in the Fermi glass regime

Figure 4. Graphs comparing the $\log T$ dependence of σ_{\square} (left) and R_{\square} (right). We analyzed two samples before and after the perpendicular flow occurred; namely (a) $\text{Nd}_2\text{CuO}_{4-x}\text{F}_x$ (NCOF) sample E in which this perpendicular flow appears and (b) NCOF sample I in which the perpendicular flow does not appear. (NCOF-sample-E is along the red arrow, and NCOF-sample-I is along the blue arrow in Fig. 3). The solid black line shows the regression line. The left vertical axis of the graph is σ_{\square} or R_{\square} . The graph's horizontal axis is $\log T$, and the right vertical axis is the value obtained by subtracting σ_{\square} or R_{\square} from the experimental value. For standardization, we divide by the value obtained by subtracting the minimum value from the maximum value of the experimental data on the vertical axis. Clearly, NCOF-sample-E is more suitable for the $\log T$ dependence of the resistivity than that of the conductivity, while NCOF-sample-I is the opposite. The perpendicular flow in the β -function indicates $\rho \sim \ln(1/T)$ rather than $\sigma \sim \ln T$. As a result, we find a difference between the $\log T$ dependence of the conductivity and resistivity. Appendix C shows graphs comparing the $\log T$ dependence of σ_{\square} and R_{\square} on other data.

that they were more suitable for $\rho \sim \ln(1/T)$ than $\sigma \sim \ln T$. However, in the ultrathin Pb film data in Fig. 5b, there were samples where the sign of $\beta'_{\text{EXP}}(g)$ changed from positive to negative when the temperature decreased. For Pb-sample-F, the sign of $\beta'_{\text{EXP}}(g)$ changed around 6 K. Since the superconducting transition temperature T_c of Pb (in the clean system) is around 7.2 K, it is conceivable that bosons are formed. On the other hand, NCOF-sample-E did not exhibit any change of sign. This may be attributed to the measurement temperature range. Another set of data measured up to the high temperature regime was analyzed, and the change was confirmed below the superconducting transition temperature T_c of the $\text{Nd}_2\text{Pd}_{1-x}\text{Cu}_x\text{O}_{4-x}\text{F}_x$ (see Appendix A).

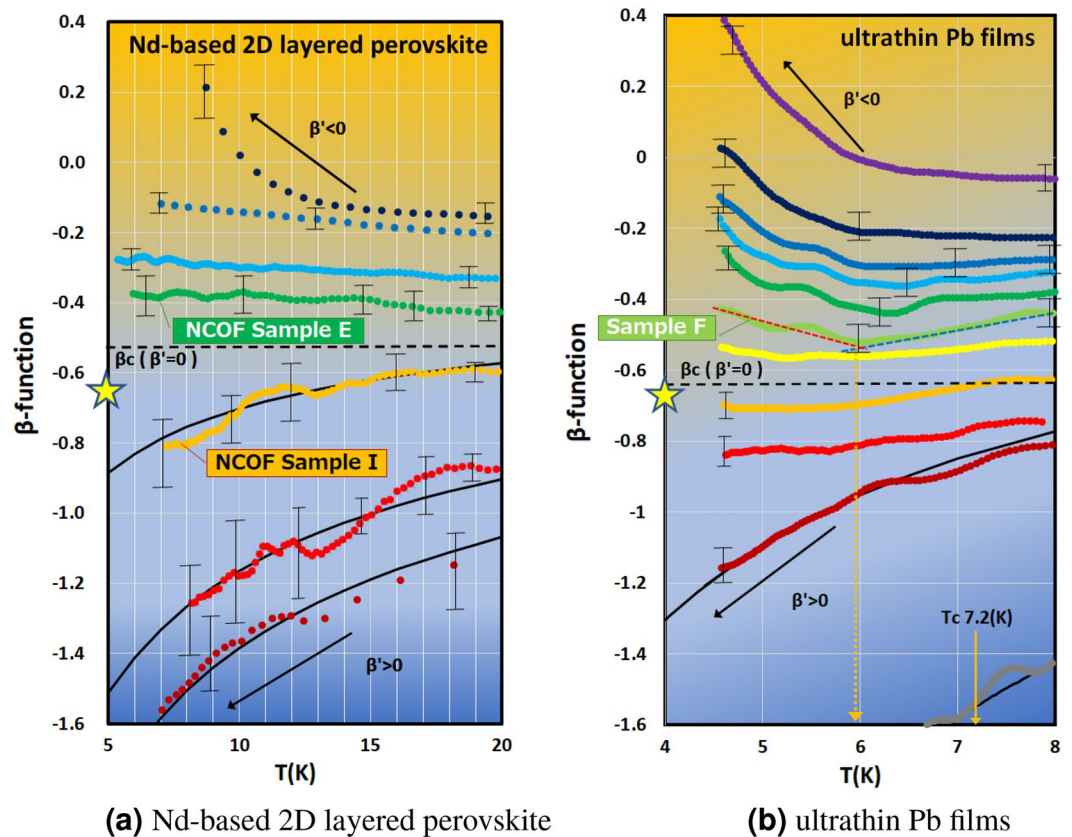


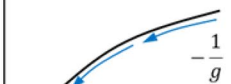
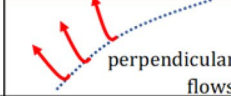
Figure 5. Graphs of the relationship between the value of $\beta_{\text{EXP}}(g)$ and temperature T with a series of experimental data in a weakly localized regime. Interestingly, the temperature dependence of $\beta_{\text{EXP}}(g)$ is very similar to the S–I transition graph. As the localization of each sample weakens (from the bottom to the top of the graph), the slope of each set of data changes continuously from positive to negative in both (a) Nd-based 2D layered perovskite and (b) ultrathin Pb films. The color depends on the sample. The solid black line shows $\beta_{\text{VW}}(g)$ —Vollhardt and Wölfle β -function [Eq. (5)]. We can see that among the weakly localized samples, those with strong localization ($\beta'_{\text{EXP}}(g) > 0$) fit into $\beta_{\text{VW}}(g)$. However, in the (b) graph, as the localization becomes weaker, the slope of Pb sample F changes from positive (blue dotted line) to negative (red dotted line) when the temperature falls below around 6 K. Since the superconducting transition temperature T_c of Pb (in a clean system) is around 7.2 K, it is conceivable that a boson appears. We also investigated the critical value of $\beta_{\text{EXP}}(g)$, denoted as β_C when the slope of $\beta'_{\text{EXP}}(g)$ goes to zero. β_C was obtained by using the slope and the intercept of the vertical axis for each sample at a specific low temperature. We obtained $\beta_C = -0.6 \pm 0.1$ in these two different types of samples. This value is almost the same $0.64 (\simeq 2/\pi)$ as shown by the yellow star, and has a value of $g = 1/2\pi$ when converted using Eq. (3). This value is the dimensionless version of the critical sheet fermion resistance $R_{\square} = h/e^2$.

We also investigated the critical value of $\beta_{\text{EXP}}(g)$, denoted as β_C , when the slope of $\beta'_{\text{EXP}}(g)$ went to zero. From Fig. 5, β_C was obtained by using the slope and the intercept of the vertical axis for each sample at a specific low temperature. We obtained $\beta_C = -0.6 \pm 0.1$ with these two different types of samples (see Appendix B). This value is almost equal to $-0.64 (\simeq -2/\pi)$ and becomes the value of $g = 1/2\pi$, which we can convert to $\beta = -2/\pi$ by using Eq. (3). The critical g does not indicate $R_{\square} = h/4e^2$ of the superconducting critical sheet resistance, but is at least close to $R_{\square} = h/e^2$ of the critical sheet fermion resistance. Mapping these values in Fig. 3 as a yellow star, we can see that the phenomenon of these perpendicular flows occurs at least when g is larger than $1/2\pi$. This $g = 1/2\pi$ value is transformed into the dimensionless version of the critical sheet fermion resistance $R_{\square} = h/e^2$. Based on the above results, at least two conditions are required to generate Bose glass; $\beta'_{\text{EXP}}(g) < 0$ and $R_{\square} < h/e^2$. The point at which the sign of $\beta'_{\text{EXP}}(g)$ changes is related to the superconducting transition temperature T_c . This experimental analysis regarding the β -function clearly demonstrated the criteria for the Fermi glass to Bose glass transition. In other words, it proved the existence of boson formation even in a localized regime.

Discussion

Finally, we suggest that the fermion-only theory may be insufficient to explain the weakly localized regime just before reaching superconductivity in 2D *disordered* superconducting materials. Fisher's theory is also insufficient because it is based on boson-only or fermion-only in the strongly localized regime represented by VRH.

Weakly localized regime in 2D disordered superconducting materials

	Function	β	β'
Fermi glass	$\sigma = \sigma_0 + \sigma_1 \ln T$		+
Bose glass	$\rho = \rho_0 + \rho_1 \ln(1/T)$		-

$\sim \frac{h}{e^2}$ (at $\beta' = 0$)

Table 1. Summary of the experimental results. In the weakly localized regime where 2D Anderson localization dominates, both Fermi glass and Bose glass exist. The existence of the Bose glass regime is clearly shown by the experimental β -function and the sign of the β' -function (the temperature derivative of the experimental β -function). We propose a universal transition from Bose glass to Fermi glass with the new two-dimensional critical sheet resistance close to $R_{\square} = h/e^2$ at $\beta' = 0$.

Meanwhile, disordered thin-film superconductors in the weakly multifractal regime can exhibit a S–I transition and allow for a boson-fermion mixture^{38–44}. The experiment using a disordered superconductor TiN revealed the existence of Cooper pairs above the superconducting transition temperature T_c ⁴⁵. Therefore, the boson-fermion mixture state and boson-only state in the weakly localized regime are important areas in clarifying the relationship between statistics (fermion, boson, and anyon) and localization. We discover an experimental renormalization group flow from Fermi glass to Bose glass by employing β -function analysis. To discuss the universality of Bose glass flow, we analyzed distinctively different systems, namely a Nd-based two-dimensional layered perovskite and an ultrathin Pb film. What these two systems have in common is that they are both 2D disordered systems, but the difference is that a Nd-based 2D layered perovskite is disordered by doping while an ultrathin Pb film is structurally disordered. Furthermore, unlike an ultrathin Pb film, a Nd-based 2D layered perovskite is a strongly correlated electron system^{9,46}. Although these two systems may have different superconductivity mechanisms, the flow of the experimental β -function exhibits the same behavior. The analysis results obtained for the two systems in common are shown in Table 1.

These results suggest the following mechanism of the crossover. With varying disorders in the weakly localized regime, Anderson localization ($\sigma \sim \ln T$) is observed when R_{\square} is larger than h/e^2 . When R_{\square} is smaller than h/e^2 , bosons and vortices are generated and the state becomes Bose glass. Furthermore, fermions disappear when R_{\square} is smaller than $h/4e^2$, and superconductivity occurs. It seems reasonable that Bose glass appears between h/e^2 and $h/4e^2$.

Paalanan et al.¹⁸ identified Bose glass as the regime where the Hall resistance ρ_{xy} has a zero or a finite value when the longitudinal resistance ρ_{xx} diverges at low temperatures and in a certain magnetic field (the bi-directional black dotted arrow in Fig. 1). On the other hand, we used the experimental β -function to identify the flow perpendicular to the 2D Anderson localized flow as Bose glass (the bi-directional red arrow in Fig. 1). This analysis constitutes a simple method of identifying weak boson/fermion localization. As an application of these results, even if superconductivity does not appear in a 2D material, the discovery of Bose glass flow in its β -function may provide a hint that could allow us to make the material superconductive by changing the disorder parameters.

Data availability

The datasets generated during and/or analyzed during the current study are available from the corresponding author on reasonable request.

Received: 29 January 2023; Accepted: 22 July 2023

Published online: 01 August 2023

References

- Anderson, P. W. *The Fermi Glass: Theory and Experiment* 353–359 (World Scientific Publishing Co Pte Ltd, 2005).
- Fleishman, L. & Anderson, P. W. Interactions and the Anderson transition. *Phys. Rev. B* **21**, 2366–2377. <https://doi.org/10.1103/PhysRevB.21.2366> (1980).
- Freedman, R. & Hertz, J. A. Theory of a fermi glass. *Phys. Rev. B* **15**, 2384–2398. <https://doi.org/10.1103/PhysRevB.15.2384> (1977).
- Abrahams, E., Kravchenko, S. V. & Sarachik, M. P. Metallic behavior and related phenomena in two dimensions. *Rev. Mod. Phys.* **73**, 251–266. <https://doi.org/10.1103/RevModPhys.73.251> (2001).
- Spivak, B., Kravchenko, S. V., Kivelson, S. A. & Gao, X. P. A. Colloquium: Transport in strongly correlated two dimensional electron fluids. *Rev. Mod. Phys.* **82**, 1743–1766. <https://doi.org/10.1103/RevModPhys.82.1743> (2010).
- Popović, D., Fowler, A. B. & Washburn, S. Metal-insulator transition in two dimensions: Effects of disorder and magnetic field. *Phys. Rev. Lett.* **79**, 1543–1546. <https://doi.org/10.1103/PhysRevLett.79.1543> (1997).
- Bogdanovich, S. C. V. & Popović, D. Onset of glassy dynamics in a two-dimensional electron system in silicon. *Phys. Rev. Lett.* **88**, 236401. <https://doi.org/10.1103/PhysRevLett.88.236401> (2002).
- Fisher, M. P. A., Grinstein, G. & Girvin, S. M. Presence of quantum diffusion in two dimensions: Universal resistance at the superconductor-insulator transition. *Phys. Rev. Lett.* **64**, 587–590. <https://doi.org/10.1103/PhysRevLett.64.587> (1990).

9. Imada, M., Fujimori, A. & Tokura, Y. Metal–insulator transitions. *Rev. Mod. Phys.* **70**, 1039–1263. <https://doi.org/10.1103/RevModPhys.70.1039> (1998).
10. Abrahams, E., Anderson, P. W., Licciardello, D. C. & Ramakrishnan, T. V. Scaling theory of localization: Absence of quantum diffusion in two dimensions. *Phys. Rev. Lett.* **42**, 673–676. <https://doi.org/10.1103/PhysRevLett.42.673> (1979).
11. Abrahams, E. *50 Years of Anderson Localization* (World Scientific, 2010).
12. Anderson, P. W. Four last conjectures (2018). <http://arxiv.org/abs/1804.11186>.
13. Lee, P. A. & Ramakrishnan, T. V. Disordered electronic systems. *Rev. Mod. Phys.* **57**, 287–337. <https://doi.org/10.1103/RevModPhys.57.287> (1985).
14. Evers, F. & Mirlin, A. D. Anderson transitions. *Rev. Mod. Phys.* **80**, 1355–1417. <https://doi.org/10.1103/RevModPhys.80.1355> (2008).
15. Obuse, H., Subramaniam, A. R., Furusaki, A., Gruzberg, I. A. & Ludwig, A. W. W. Conformal invariance, multifractality, and finite-size scaling at Anderson localization transitions in two dimensions. *Phys. Rev. B* **82**, 035309. <https://doi.org/10.1103/PhysRevB.82.035309> (2010).
16. Gruzberg, I. A., Read, N. & Vishveshwara, S. Localization in disordered superconducting wires with broken spin-rotation symmetry. *Phys. Rev. B* **71**, 245124. <https://doi.org/10.1103/PhysRevB.71.245124> (2005).
17. Fisher, M. P. A., Weichman, P. B., Grinstein, G. & Fisher, D. S. Boson localization and the superfluid–insulator transition. *Phys. Rev. B* **40**, 546–570. <https://doi.org/10.1103/PhysRevB.40.546> (1989).
18. Paalanen, M. A., Hebard, A. F. & Ruel, R. R. Low-temperature insulating phases of uniformly disordered two-dimensional superconductors. *Phys. Rev. Lett.* **69**, 1604–1607. <https://doi.org/10.1103/PhysRevLett.69.1604> (1992).
19. Evers, F. & Mirlin, A. D. Anderson transitions. *Rev. Mod. Phys.* **80**, 1355–1417 (2008).
20. Mott, N. F. Conduction in non-crystalline materials. *Philos. Mag.* **19**, 835–852 (1969).
21. Fisher, M. P. A. Quantum phase transitions in disordered two-dimensional superconductors. *Phys. Rev. Lett.* **65**, 923–926. <https://doi.org/10.1103/PhysRevLett.65.923> (1990).
22. Haldar, P., Laad, M. S. & Hassan, S. R. Quantum critical transport at a continuous metal–insulator transition. *Phys. Rev. B* **94**, 081115. <https://doi.org/10.1103/PhysRevB.94.081115> (2016).
23. Kapitulnik, A., Kivelson, S. A. & Spivak, B. Colloquium: Anomalous metals: Failed superconductors. *Rev. Mod. Phys.* **91**, 011002. <https://doi.org/10.1103/RevModPhys.91.011002> (2019).
24. Haviland, D. B., Liu, Y. & Goldman, A. M. Onset of superconductivity in the two-dimensional limit. *Phys. Rev. Lett.* **62**, 2180–2183. <https://doi.org/10.1103/PhysRevLett.62.2180> (1989).
25. Müller-Buschbaum, H. & Wollschläger, M. Über ternäre oxocuprate. vii. Zur kristallstruktur von Nd₂CuO₄. *Z. Anorg. Allgem. Chem.* **414**, 76–80 (1975).
26. Tanda, S., Takahashi, K. & Nakayama, T. Scaling behavior of the conductivity of Nd₂CuO_{4-x}δF_x single crystals: Evidence for orthogonal symmetry. *Phys. Rev. B* **49**, 9260–9263. <https://doi.org/10.1103/PhysRevB.49.9260> (1994).
27. Tanda, S., Honma, M. & Nakayama, T. Critical sheet resistance observed in high-T_c oxide-superconductor Nd₂CuO₄ thin films. *Phys. Rev. B* **43**, 8725–8728. <https://doi.org/10.1103/PhysRevB.43.8725> (1991).
28. Nanao, Y. *et al.* Crystal growth and metal–insulator transition in two-dimensional layered rare-earth palladates. *Phys. Rev. Mater.* **2**, 085003. <https://doi.org/10.1103/PhysRevMaterials.2.085003> (2018).
29. Kagawa, K., Inagaki, K. & Tanda, S. Superconductor–insulator transition in ultrathin Pb films: Localization and superconducting coherence. *Phys. Rev. B* **53**, R2979–R2982. <https://doi.org/10.1103/PhysRevB.53.R2979> (1996).
30. Hill, R. M. On the observation of variable range hopping. *Phys. Status Solidi A* **35**, K29–K34 (1976).
31. Vollhardt, D. & Wölfle, P. Scaling equations from a self-consistent theory of Anderson localization. *Phys. Rev. Lett.* **48**, 699–702. <https://doi.org/10.1103/PhysRevLett.48.699> (1982).
32. Wölfle, P. & Vollhardt, D. *Self-consistent Theory of Anderson Localization: General Formalism and Applications* 43–71 (World Scientific, Singapore, 2010).
33. Dobrosavljević, V., Abrahams, E., Miranda, E. & Chakravarty, S. Scaling theory of two-dimensional metal–insulator transitions. *Phys. Rev. Lett.* **79**, 455–458. <https://doi.org/10.1103/PhysRevLett.79.455> (1997).
34. Kravchenko, S. V., Simonian, D., Sarachik, M. P., Mason, W. & Furneaux, J. E. Electric field scaling at a B = 0 metal–insulator transition in two dimensions. *Phys. Rev. Lett.* **77**, 4938–4941. <https://doi.org/10.1103/PhysRevLett.77.4938> (1996).
35. Finkel'shtein, A. Influence of coulomb interaction on the properties of disordered metals. *J. Exp. Theor. Phys.* **57**, 97–108 (1983).
36. Finkel'shtein, A. Weak localization and coulomb interaction in disordered systems. *Z. Phys. B Condens. Matter* **56**, 189–196. <https://doi.org/10.1007/BF01304171> (1984).
37. Das, D. & Doniach, S. Weakly localized bosons. *Phys. Rev. B* **57**, 14440–14443. <https://doi.org/10.1103/PhysRevB.57.14440> (1998).
38. Feigel'man, M. V., Ioffe, L. B., Kravtsov, V. E. & Cuevas, E. Fractal superconductivity near localization threshold. *Ann. Phys.* **325**, 1390–1478. <https://doi.org/10.1016/j.aop.2010.04.001> (2010) (110 pages, 39 figures).
39. Burmistrov, I. S., Gornyi, I. V. & Mirlin, A. D. Enhancement of the critical temperature of superconductors by Anderson localization. *Phys. Rev. Lett.* **108**, 017002. <https://doi.org/10.1103/PhysRevLett.108.017002> (2012).
40. Burmistrov, I. S., Gornyi, I. V. & Mirlin, A. D. Superconductor–insulator transitions: Phase diagram and magnetoresistance. *Phys. Rev. B* **92**, 014506. <https://doi.org/10.1103/PhysRevB.92.014506> (2015).
41. Stosiek, M., Evers, F. & Burmistrov, I. S. Multifractal correlations of the local density of states in dirty superconducting films. *Phys. Rev. Res.* **3**, 206. <https://doi.org/10.1103/physrevresearch.3.042016> (2021).
42. Sacépé, B., Feigel'man, M. & Klapwijk, T. M. Quantum breakdown of superconductivity in low-dimensional materials. *Nat. Phys.* **16**, 734–746. <https://doi.org/10.1038/s41567-020-0905-x> (2020).
43. Cyr-Choinière, O. *et al.* Pseudogap temperature T* of cuprate superconductors from the nernst effect. *Phys. Rev. B* **97**, 064502. <https://doi.org/10.1103/PhysRevB.97.064502> (2018).
44. Behnia, K. & Aubin, H. Nernst effect in metals and superconductors: A review of concepts and experiments. *Rep. Progress Phys.* **79**, 046502. <https://doi.org/10.1088/0034-4885/79/4/046502> (2016).
45. Bastiaans, K. M. *et al.* Direct evidence for cooper pairing without a spectral gap in a disordered superconductor above T_c. *Science* **374**, 608–611. <https://doi.org/10.1126/science.abe3987> (2021).
46. Naito, M., Krockenberger, Y., Ikeda, A. & Yamamoto, H. Reassessment of the electronic state, magnetism, and superconductivity in high-tc cuprates with the nd2cuo4 structure. *Physica C* **523**, 28–54. <https://doi.org/10.1016/j.physc.2016.02.012> (2016).

Acknowledgements

We are grateful to K. Yakubo, K. Ichimura and T. Matsuyama for suggesting the topic dealt with in this Article. We thank M. Naito for his help in preparing the experimental Nd_{2-x}Ce_xPdO₄ samples. We also thank many of those who attended the Forum of Localisation 2020. We have gained useful insights. Finally, we would like to thank S. Ozeki, K. Kagawa and K. Inagaki who studied together about 30 years ago, and T. Nakayama for introducing such a wonderful physics field.

Author contributions

Conceptualization, S.T. and K.T.; methodology, S.T., K.T. and K.N.; software, K.T., K.N.; validation, K.T., K.N. and S.T.; formal analysis, K.T., K.N. and S.T.; investigation, K.T. and Y.N.; resources, K.T., Y.N. and M.S.; data curation, K.T.; writing-original draft preparation, K.T.; writing-review and editing, S.T., H.N., K.T., H.O. and K.N.; visualization, K.T. and K.N.; supervision, S.T.; project administration, S.T.; funding acquisition, S.T. All authors have read and agreed to the published version of the manuscript.

Competing interests

The authors declare no competing interests.

Additional information

Supplementary Information The online version contains supplementary material available at <https://doi.org/10.1038/s41598-023-39285-1>.

Correspondence and requests for materials should be addressed to K.T.

Reprints and permissions information is available at www.nature.com/reprints.

Publisher's note Springer Nature remains neutral with regard to jurisdictional claims in published maps and institutional affiliations.



Open Access This article is licensed under a Creative Commons Attribution 4.0 International License, which permits use, sharing, adaptation, distribution and reproduction in any medium or format, as long as you give appropriate credit to the original author(s) and the source, provide a link to the Creative Commons licence, and indicate if changes were made. The images or other third party material in this article are included in the article's Creative Commons licence, unless indicated otherwise in a credit line to the material. If material is not included in the article's Creative Commons licence and your intended use is not permitted by statutory regulation or exceeds the permitted use, you will need to obtain permission directly from the copyright holder. To view a copy of this licence, visit <http://creativecommons.org/licenses/by/4.0/>.

© The Author(s) 2023